

Phys. Chem. Res., Vol. 2, No. 2, 171-178, December 2014.

DOI: 10.22036/pcr.2014.5540

Interplay Between Lithium Bonding and Halogen Bonding in $F_3CX \cdots YLi \cdots NCCN$ and $F_3CX \cdots NCCN \cdots LiY$ Complexes (X = Cl, Br; Y = CN, NC)

M. Solimannejad*, E. Bayatmanesh and M.D. Esrafil

Department of Chemistry, Faculty of Sciences, Arak University, Arak 38156-8-8349, Iran

Laboratory of Theoretical Chemistry, Department of Chemistry, University of Maragheh, Maragheh, Iran

(Received 11 February 2014, Accepted 18 May 2014)

MP2 calculations with cc-pVTZ basis set were used to analyze intermolecular interactions in $F_3CX \cdots YLi \cdots NCCN$ and $F_3CX \cdots NCCN \cdots LiY$ triads (X = Cl, Br; Y = CN, NC) which are connected *via* halogen and lithium bonds. Those complexes with the role of LiY as halogen acceptor and lithium donor show cooperativity with energy values ranging between -1.97 and -2.92 kJ mol⁻¹. Those complexes with simultaneous role of NCCN as halogen and lithium acceptor are diminutive with energetic effects between 1.24 and 1.86 kJ mol⁻¹. Results of energy decomposition analysis revealed that the electrostatic interactions are the major source of the attraction in the title complexes. The nuclear quadrupole coupling constant values at the sites of halogen atoms can be regarded as good descriptors to quantify the degree of cooperative/diminutive effects in the title systems.

Keywords: Cooperativity, Halogen bonds, Lithium bonding, EDA, NQR

INTRODUCTION

Noncovalent interactions between molecules play a very important role in supramolecular chemistry, molecular biology, and materials science [1]. Although research has traditionally focused on the most common hydrogen bond interactions, more recently, interest has grown for other types of intermolecular interactions, such as lithium and halogen bonds.

Lithium bond is an interesting interaction analogous to hydrogen bond [2-7]. The common feature of these two interactions is that both the hydrogen and lithium atoms possess a single electron in a valence *s* orbital. The existence of lithium bonding was first suggested as a possibility by Shigorin in 1959 [8], and was theoretically predicted in 1970 by Kollman *et al.* [9]. Then, in 1975, Ault and Pimentel [10] provided the experimental evidence for lithium bonding, *i.e.*, a large red shift of the Li-Y stretching

frequency in $X \cdots Li-Y$ complexes (X = H₃N, Me₃N, H₂O, Me₂O; Y = Cl, Br). To date, lithium bonds have been identified in a variety of systems and the concept of lithium bonding has become important in many fields. Lithium bond interactions play a crucial role in supramolecular chemistry [11]. However, studies on lithium bond interactions far smaller than that of hydrogen bond [12-20].

Halogen bonding (XB) has drawn more and more attention because of its potential applications in molecular recognition [21-23], crystal engineering [24-26] and biological systems [27-30]. Halogen bonding is a type of noncovalent interaction between a halogen atom X in one molecule and a negative site in another [31-35]. There is a sigma-hole on the outer surface of a covalently-bonded halogen atom, which can be evidenced from molecular electrostatic potentials [36].

The cooperative (or many-body) effects in intermolecular interactions play a critical role in the modern view of condensed matter [37]. It is typically described as non-additive enhancement of an interaction through formation of another one. Thus, the strength of hydrogen

*Corresponding authors. E-mail: m-solimannejad@araku.ac.ir

bonds in clusters usually increases as further molecules are added; also, the frequencies of some vibrational modes are shifted by effect of the incorporation of new molecules [38].

Careful studies in simple models are of interest in order to extend their conclusion to larger ones. Herein, we designed some simple structures including halogen and lithium bonds. In this article, we thus constructed $F_3CX \cdots YLi \cdots NCCN$ and $F_3CX \cdots NCCN \cdots LiY$ triads ($X = Cl, Br$; $Y = CN, NC$) where two types of bonding coexist. To our best knowledge, study of cooperativity in triads with lithium and halogen bonds in literature is rare [12,16].

COMPUTATIONAL DETAILS

Structures of the monomers and the complexes have been optimized and characterized by frequency computations at the MP2/cc-pVTZ computational level. Riley *et al.* pointed out that this method provides very good estimates of geometries and energies for noncovalent complexes [39]. The interaction energies were calculated as the difference between the total energy of the complexes and the sum of the isolated monomers in their minima configuration. The full counterpoise (CP) method [40] was used to correct the interaction energy from the inherent basis set superposition error (BSSE). To gain a deeper insight into the nature of the interactions, in terms of meaningful physical components, interaction energies were decomposed using the following partitioning of interaction energy components [41]:

$$E_{\text{int}} = E_{\text{elst}} + E_{\text{exch-rep}} + E_{\text{pol}} + E_{\text{disp}} \quad (1)$$

where E_{elst} is the electrostatic term describing the classical Coulomb interaction of the occupied orbitals of one monomer with those of another monomer, $E_{\text{exch-rep}}$ is the repulsive exchange component resulting from the Pauli exclusion principle. E_{pol} and E_{disp} correspond to polarization and dispersion terms, respectively. The polarization term contains all classical induction, exchange-induction, *etc.*, from the second order up to infinity.

In nuclear quadrupole resonance (NQR) spectroscopy, the interaction between nuclear electric quadrupole moment and electric field gradient (EFG) at quadrupole nucleus is described with Hamiltonian as follows [42]:

$$\hat{H} = \frac{e^2 Q q_{zz}}{4I(2I-1)} [(3\hat{I}_z^2 - \hat{I}^2) + \eta_Q (\hat{I}_x^2 - \hat{I}_y^2)] \quad (2)$$

where eQ is the nuclear electric quadrupole moment, I is the nuclear spin, and q_{zz} is the largest component of the EFG tensor. The principal components of the EFG tensor, q_{ii} , are computed in atomic unit ($1 \text{ au} = 9.717365 \times 10^{21} \text{ V m}^{-2}$), with $|q_{zz}| \geq |q_{yy}| \geq |q_{xx}|$ and $q_{xx} + q_{yy} + q_{zz} = 0$. These diagonal elements relate to each other by the asymmetry parameter: $\eta_Q = |q_{yy} - q_{xx}|/|q_{zz}|$, $0 \leq \eta_Q \leq 1$, that measures the deviation of EFG tensor from axial symmetry. The computed q_{zz} component of EFG tensor is used to obtain the nuclear quadrupole coupling constant from the equation; $C_Q(\text{MHz}) = e^2 Q q_{zz}/h$, using the recently reported value for the ^{35}Cl and ^{79}Br electric quadrupole moments of -81.65 and 313 mb, respectively [43].

All geometry optimizations, interaction energies and energy components were calculated using GAMESS package [44].

RESULTS AND DISCUSSION

Geometries

The intermolecular distances found for these systems are in the range of 2.90-3.25 Å for $X \cdots N(\text{C})$ halogen bonds and 2.070-2.078 for $\text{Li} \cdots \text{N}$ lithium bonds (Table 1). These are shorter than the sum of the van der Waals (vdW) radii of the atoms involved ($r_{\text{vdw,C}} = 1.70 \text{ \AA}$, $r_{\text{vdw,N}} = 1.55 \text{ \AA}$, $r_{\text{vdw,Li}} = 1.82 \text{ \AA}$, $r_{\text{vdw,Cl}} = 1.75 \text{ \AA}$ and $r_{\text{vdw,Br}} = 1.85 \text{ \AA}$) [45], which implies that there is an attractive force between the two subunits.

For the systems with $F_3CX \cdots YLi \cdots NCCN$ arrangement, the $X \cdots N(\text{C})$ and $\text{Li} \cdots \text{N}$ distances in the triads are smaller than the corresponding values in the dyads, with differences in the range between 0.011 to 0.028 Å and 0.003 to 0.006 Å, respectively. That is, the two types of interaction have a cooperative effect on each other. For systems with $F_3CX \cdots NCCN \cdots LiY$ arrangement, the $X \cdots N$ and $\text{Li} \cdots \text{N}$ distances in the triads are larger than the corresponding values in the dyads, with differences in the range between 0.068 to 0.077 Å and 0.001 Å respectively (Table 1). This trend can be interpreted as a diminutive effect of lithium and halogen bonds.

Interaction Energies

The interaction energy in the dyads can be regarded as

Table 1. Intermolecular Distances R (in Å) in the Investigated Triads (T), and Dyads. ΔR Indicates the Changes Relative to the Respective Dyads

Triads(A...B...C)	R(AB,T)	R(AB,D)	$\Delta R(AB)$	R(BC,T)	R(BC,D)	$\Delta R(BC)$
F ₃ CCl...NCLi...NCCN	2.968	2.985	-0.017	2.072	2.076	-0.004
F ₃ CCl...CNLi...NCCN	3.113	3.124	-0.011	2.072	2.076	-0.003
F ₃ CBr...NCLi...NCCN	2.907	2.927	-0.020	2.070	2.076	-0.006
F ₃ CBr...CNLi...NCCN	2.997	3.026	-0.028	2.070	2.076	-0.005
F ₃ CCl...NCCN...LiCN	3.251	3.181	0.069	2.076	2.076	0.000
F ₃ CCl...NCCN...LiNC	3.250	3.181	0.068	2.076	2.076	0.000
F ₃ CBr...NCCN...LiCN	3.247	3.170	0.076	2.078	2.076	0.001
F ₃ CBr...NCCN...LiNC	3.247	3.170	0.077	2.077	2.076	0.001

Table 2. Interaction Energies E_{int} (kJ mol⁻¹) of Halogen and Lithium Bonding in the Studied Dyads and Triads (T) at MP2/cc-pVTZ

Triads(A...B...C)	$E_{\text{int}}(ABC)$	$E_{\text{int}}(AB)$	$E_{\text{int}}(BC)$	$E_{\text{int}}(AB,T)$	$E_{\text{int}}(BC,T)$	E_{coop}	E_{syn}
F ₃ CCl...NCLi...NCCN	-67.07	-12.70	-53.23	-12.50	-53.21	-1.97	-1.13
F ₃ CCl...CNLi...NCCN	-66.74	-12.27	-53.27	-12.08	-53.25	-2.01	-1.19
F ₃ CBr...NCLi...NCCN	-73.20	-18.24	-53.23	-17.98	-53.19	-2.70	-1.72
F ₃ CBr...CNLi...NCCN	-73.76	-18.63	-53.27	-18.30	-53.21	-2.92	-1.85
F ₃ CCl...NCCN...LiCN	-56.41	-4.98	-53.23	-4.78	-53.23	1.25	1.80
F ₃ CCl...NCCN...LiNC	-56.43	-4.98	-53.27	-4.79	-53.27	1.24	1.83
F ₃ CBr...NCCN...LiCN	-57.41	-6.77	-53.23	-6.63	-53.23	1.86	2.60
F ₃ CBr...NCCN...LiNC	-57.42	-6.77	-53.27	-6.63	-53.28	1.86	2.63

the energy difference between the complex and the monomers: $E_{\text{int}}(AB) = E_{AB} - (E_A + E_B)$ and the corresponding value in the triads ($E_{\text{int}}(ABC)$) are calculated in a similar way. $E_{\text{int}}(AB,T)$ and $E_{\text{int}}(BC,T)$ are the interaction energies of AB and BC dyads while they are in the geometry of triads (T is used to denote geometry of triads). In Table 2, the interaction energy of the eight studied triads and respective dyads are presented. All results were corrected for BSSE using the CP method. As shown in Table 2, the interaction energy of the title complexes ranges from -56.4 to -73.7 kJ mol⁻¹.

For the complexes in which halogen bonds and lithium interactions coexist, the cooperativity energy E_{coop} was evaluated using Eq. (3) [46]:

$$E_{\text{coop}} = E_{\text{int}}(ABC) - E_{\text{int}}(AB) - E_{\text{int}}(BC) - E_{\text{int}}(AC,T) \quad (3)$$

where $E_{\text{int}}(ABC)$ is the interaction energy of the triads, $E_{\text{int}}(AB)$ and $E_{\text{int}}(BC)$ are the interaction energies of the isolated dimers within their corresponding minima configuration and $E_{\text{int}}(AC,T)$ is interaction energy of an imaginary dimer formed between A and C in geometry of triads. We also calculated the synergetic energies (E_{syn}) using the first three terms of Eq. (3) [46]. An important finding is that the complexes with strong halogen bond interactions exhibit strong synergic effects, while much weak cooperativity occurs in the F₃CCl...NCLi...NCCN complex. In F₃CX...YLi...NCCN complexes, a favorable

cooperativity effect is also observed with values ranging between -1.97 to -2.92 kJ mol⁻¹. In the same way, diminutive effects are evident for those complexes with F₃CX...NCCN...LiY arrangement in the ranges between 1.24 to 1.86 kJ mol⁻¹. The results of calculated synergetic energies are in line with results of cooperativity in the studied complexes.

Many-Body Interaction Analysis

To further understand the cooperativity effects in the title complexes, we performed an analysis of many-body decomposition of the interaction energy [47,48]. The total interaction energy of the ABC triad equals to the sum of the relaxation energy and many-body terms:

$$E_{\text{int}}(\text{ABC}) = E_{\text{R}} + E_{\text{int A-B}} + E_{\text{int A-C}} + E_{\text{int B-C}} + E_{\text{int A-B-C}} \quad (4)$$

The relaxation energy (E_{R}) is defined as the energy sum of the monomers frozen in the geometry of the triads minus the energy sum of the optimized monomers. The two-body terms ($E_{\text{int A-B}}$, $E_{\text{int B-C}}$, and $E_{\text{int A-C}}$) can be calculated as the interaction energy of each molecular pair in the geometry of triad minus the energy sum of the monomers, all of them are frozen in the geometry of the triad. The three-body term $E_{\text{int A-B-C}}$ is calculated as the interaction energy of the triad minus the interaction energy of each pair of monomers, all of them are frozen in the geometry of the triad using Eq. (5) [49]:

$$E_{\text{int A-B-C}} = E_{\text{int}}(\text{ABC})' - E_{\text{int A-B}} - E_{\text{int A-C}} - E_{\text{int B-C}} \quad (5)$$

$E_{\text{int}}(\text{ABC})'$ is obtained by subtracting total energy of optimized triads from the energy sum of the monomers frozen in the geometry of the triads.

The results are presented in Table 3, in which all energies are corrected for BSSE. As seen in Table 3, A-B and B-C, two-body interaction energy provides the largest contribution of the total interaction energy. For all the ternary complexes, the two-body and three-body interaction energies are attractive, indicating a positive contribution to the stabilization energy of complexes. For all triads $E_{\text{int A-C}}$ is the smallest two-body interaction term which is consistent with the largest distance between them. Analysis results of

Table 3 reveals that contribution of lithium bonding in stability of title triads is more than that of halogen bonding.

The relaxation energy E_{R} can be taken as a measure of the degree of strain that drives the distortion of the ternary system. As seen in Table 3, the relaxation energy is positive, so makes a destabilizing contribution to the total interaction energy of the triads.

Energy Decomposition Analysis

Insights into the origin and nature of the interactions in title triads can be found from a partitioning of the interaction energy into different contributions. It may be noted that there is no rigorous basis for defining such energy terms [50], since they are not physical observable quantities. The energy components are not independent of each other, no matter what procedure is used. Although all of the energy partition schemes are arbitrary, they can provide chemical insights into energetic differences when they are applied to an analogous series of complexes, as in this case.

The results of energy decomposition for the title complexes are given in Table 4. It is revealed that the attractive electrostatic and polarization components make the major contribution to the interaction energies. According to the energy decomposition results, it is also found that electrostatic effects account for 61-63% of the overall attraction in all the studied triads. By comparison, the polarization component of these interactions represents 28-32% of the total attractive forces. This reveals that the electrostatic interactions are essentially responsible for the stability of the title triads.

Considering the electrostatic nature of the interactions, the electrostatic potentials at the 0.001 electrons/Bohr³ isodensity surfaces of the F₃CX, LiY and NCCN monomers as well as the corresponding dyads were computed by means of the WFA (wave function analysis) surface analysis suite [52,53]. Figure 1 indicates the electrostatic potential map of the isolated F₃CX, LiY and NCCN molecules. Table 5 lists the magnitudes of the most positive ($V_{\text{S,max}}$) and most negative electrostatic potentials ($V_{\text{S,min}}$) on the surface of these molecules. The $V_{\text{S,max}}$ is 214 kcal mol⁻¹ in CF₃Br...NCLi complex, which is more positive than that in LiCN isolated monomer. This indicates that the Li atom in the CF₃Br...NCLi dyad is a stronger electron acceptor

Table 3. Decomposition of Stabilization Energy (kJ mol^{-1}) of the Studied Triads Using the Geometry within the Triads

Triads(A...B...C)	$E_{\text{int A-B}}$	$E_{\text{int B-C}}$	$E_{\text{int A-C}}$	$E_{\text{int A-B-C}}$	E_{R}
$\text{F}_3\text{CCl}\cdots\text{NCLi}\cdots\text{NCCN}$	-13.51	-53.62	-0.15	-0.98	1.19
$\text{F}_3\text{CCl}\cdots\text{CNLi}\cdots\text{NCCN}$	-13.12	-53.70	-0.15	-0.99	1.23
$\text{F}_3\text{CBr}\cdots\text{NCLi}\cdots\text{NCCN}$	-19.23	-53.65	-0.21	-1.54	1.44
$\text{F}_3\text{CBr}\cdots\text{CNLi}\cdots\text{NCCN}$	-19.77	-53.77	-0.21	-1.65	1.66
$\text{F}_3\text{CCl}\cdots\text{NCCN}\cdots\text{LiCN}$	-4.97	-53.54	0.43	1.36	0.30
$\text{F}_3\text{CCl}\cdots\text{NCCN}\cdots\text{LiNC}$	-4.97	-53.60	0.44	1.37	0.32
$\text{F}_3\text{CBr}\cdots\text{NCCN}\cdots\text{LiCN}$	-6.81	-53.53	0.62	2.02	0.30
$\text{F}_3\text{CBr}\cdots\text{NCCN}\cdots\text{LiNC}$	-6.81	-53.59	0.63	2.03	0.31

Table 4. Calculated Interaction Energy Components (in kJ mol^{-1}) for the Title Complexes

Triads (A...B...C)	E_{elst}	$E_{\text{exch-rep}}$	E_{pol}	E_{disp}
$\text{F}_3\text{CCl}\cdots\text{NCLi}\cdots\text{NCCN}$	-16.87	10.22	-8.51	-1.43
$\text{F}_3\text{CCl}\cdots\text{CNLi}\cdots\text{NCCN}$	-17.06	11.26	-8.25	-2.37
$\text{F}_3\text{CBr}\cdots\text{NCLi}\cdots\text{NCCN}$	-19.92	13.81	-9.99	-2.02
$\text{F}_3\text{CBr}\cdots\text{CNLi}\cdots\text{NCCN}$	-21.43	16.91	-10.25	-3.33
$\text{F}_3\text{CCl}\cdots\text{NCCN}\cdots\text{LiCN}$	-12.67	6.85	-6.25	-1.43
$\text{F}_3\text{CCl}\cdots\text{NCCN}\cdots\text{LiNC}$	-12.48	6.9	-6.00	-1.92
$\text{F}_3\text{CBr}\cdots\text{NCCN}\cdots\text{LiCN}$	-13.20	7.51	-6.26	-1.78
$\text{F}_3\text{CBr}\cdots\text{NCCN}\cdots\text{LiNC}$	-13.02	7.57	-6.02	-2.27

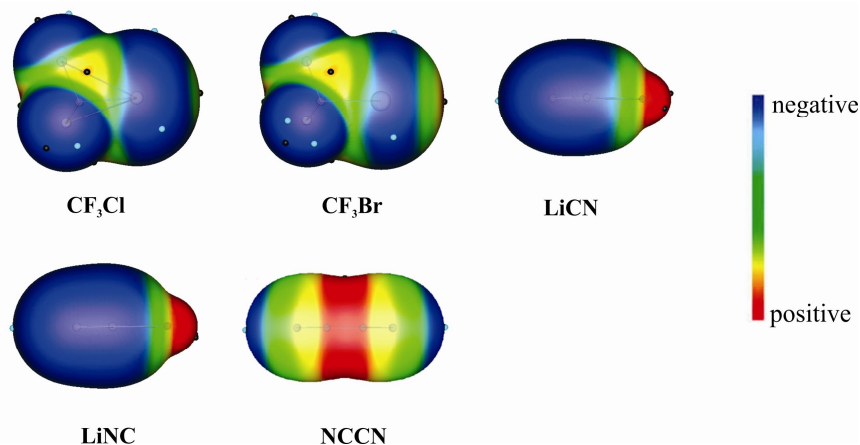
**Fig. 1.** Electrostatic potential maps at the 0.001 electron/Bohr³ isodensity surface of isolated CF_3Cl , CF_3Br , LiCN , LiNC and NCCN molecules. Black and blue circles are surface maxima and minima, respectively.

Table 5. The most Positive ($V_{S,max}$, kJ mol⁻¹) and most Negative ($V_{S,min}$, kJ mol⁻¹) Electrostatic Potentials in the Monomers and the Corresponding Dyads

Molecule	$V_{S,max}$	$V_{S,min}$
F ₃ CCl	91.9	-16.7
F ₃ CBr	121.2	-16.7
NCCN	848.5	-238.2
LiCN	873.6	-254.9
LiNC	848.5	-238.2
F ₃ CCl...NCCN	146.0	-71.0
F ₃ CBr...NCCN	150.4	-71.0
F ₃ CCl...NCLi	886.1	-183.9
F ₃ CBr...NCLi	894.5	-171.3
F ₃ CCl...CNLi	861.0	-150.4
F ₃ CBr...CNLi	869.4	-129.5
NCLi...NCCN	572.6	-275.8
CNLi...NCCN	555.9	-254.9

Table 6. Calculated Nuclear Quadrupole Coupling Constants C_Q in Triads (T) and Dyads. All C_Q Values are in MHz. ΔC_Q Indicates the Changes Relative to the Respective Dyads

Triads (A...B...C)	C_Q	$C_Q(T)$	ΔC_Q
F ₃ CCl...NCLi...NCCN	79.86	80.19	0.33
F ₃ CCl...CNLi...NCCN	79.77	80.08	0.31
F ₃ CBr...NCLi...NCCN	604.98	609.24	4.26
F ₃ CBr...CNLi...NCCN	606.22	611.02	4.80
F ₃ CCl...NCCN...LiCN	77.20	76.34	-0.86
F ₃ CCl...NCCN...LiNC	77.20	76.37	-0.83
F ₃ CBr...NCCN...LiCN	574.52	565.52	-9.00
F ₃ CBr...NCCN...LiNC	574.52	565.76	-8.76

than that of free LiCN molecule, which would enhance the attraction between this dyad and the NCCN molecule. This is also in agreement with the cooperative effects between the Br...N and Li...N interactions in this complex. On the other hand, when NCCN interacts with the CF₃X or LiY molecule, $V_{S,min}$ on the N atom becomes less negative. These results reveal that the electrostatic interaction is a dominant factor in cooperative/diminutive effects between the both types of interactions.

Nuclear Quadrupole Coupling Constants

In Table 6, the nuclear quadrupole coupling constants (C_Q) at the sites of ³⁵Cl and ⁷⁹Br nuclei of the dyads and triads are listed. In NQR spectroscopy, the interaction between nuclear electric quadrupole moments, eQ, of quadrupolar nuclei (having spin $I > 1/2$) with local molecular electric field gradient, EFG, has the characteristic role [43]. Nuclear quadrupole coupling constant, C_Q , determine eQ interaction amount with EFG. EFG at a

nucleus in molecular environments is the expectation value of a one-electron operator and can be obtained with a reasonable effort using theoretical calculations. As it only involves the ground state wave function, C_Q calculation is easier and faster than calculation of nuclear magnetic resonance (NMR) parameters such as chemical shielding and spin-spin coupling constants.

The calculated C_Q values of CF_3Cl and CF_3Br monomers are about 76.5 and 565.2 MHz, respectively. The MP2/cc-pVTZ calculations reveal that the formation of complexes results in a significant shift in the C_Q values. In particular, the results indicate that the C_Q values at the site of Br atoms are increased by 9.32-41.02 MHz from the monomer to the binary systems. Cooperative effects strengthen the halogen bond interactions and therefore lead to considerable shifts in C_Q values. For systems with $\text{F}_3\text{CX}\cdots\text{YLi}\cdots\text{NCCN}$ arrangement, the ΔC_Q in the triads are larger than that in the dyads. Obviously, the amount of ΔC_Q depends on the strength of halogen bonds and lithium bond interactions. It is largest for $\text{F}_3\text{CBr}\cdots\text{CNLi}\cdots\text{NCCN}$ and smallest for the $\text{F}_3\text{CCl}\cdots\text{CNLi}\cdots\text{NCCN}$. For a given Y, the ΔC_Q value increases in the order chloride bond < bromide bond, which is consistent with the shorter intermolecular distance and the greater amount of positive electrostatic potential on the halogen atom. On the other hand, for systems with $\text{F}_3\text{CX}\cdots\text{NCCN}\cdots\text{LiY}$ configuration, the estimated C_Q values in the triads are smaller than the corresponding values in the dyads, with differences in the range between 0.83 to 9.00 MHz (Table 6). This trend can be interpreted as a diminutive effect of halogen bond and lithium bond interaction. The effect is larger in those complexes with stronger intermolecular interactions than in those with the weaker ones. This finding supports the view that the degree of cooperativity is proportional to strength of the intermolecular interactions. This reveals that the ΔC_Q values at the sites of halogen atoms can be regarded as a good description to quantify the degree of cooperative/diminutive effects in the title systems.

CONCLUSIONS

The $\text{F}_3\text{CX}\cdots\text{YLi}\cdots\text{NCCN}$ and $\text{F}_3\text{CX}\cdots\text{NCCN}\cdots\text{LiY}$ triads (X = Cl, Br; Y = CN, NC) were investigated with quantum chemical calculations at the MP2/cc-pVTZ level. The equilibrium structures and cooperative effect on the

properties of the complexes were analyzed. The triads with the NCCN molecule located at the end of the chain showed energetic cooperativity. When the NCCN molecule was located in the middle, the obtained cluster was diminutive. Nuclear quadrupole coupling constants values at the sites of halogen atoms can be regarded as a good description to quantify the degree of cooperative/diminutive effects in the title systems. These findings are helpful for understanding the cooperative and competitive role of lithium and halogen bonding in molecular recognition, crystal engineering and biological systems.

REFERENCES

- [1] K. Müller-Dethlefs, P. Hobza, *Chem. Rev.* 100 (2000) 143.
- [2] Z. Latajka, S. Scheiner, *J. Chem. Phys.* 81 (1984) 4014.
- [3] M.M. Szczesniak, P. Hobza, Z. Latajka, H. Ratajczak, K. Skowronek, *J. Phys. Chem.* 88 (1984) 5923.
- [4] Z. Latajka, H. Ratajczak, K. Morokuma, W.J. Orville-Thomas, *J. Mol. Struct.* 146 (1986) 263.
- [5] Y. Bouteiller, Z. Latajka, H. Ratajczak, S. Scheiner, *J. Chem. Phys.* 94 (1991) 2956.
- [6] S. Salai, C. Ammala, P. Venuvanalingam, *J. Chem. Phys.* 109 (1998) 9820.
- [7] S. Scheiner, E.A.M. Sapse, P.R. Schreiner, *Recent Studies in Lithium Chemistry: A Theoretical and Experimental Overview*, John Wiley & Sons Inc., New York, 1995.
- [8] D.N. Shigorin, *Spectrochim. Acta* 14 (1959) 198.
- [9] P.A. Kollman, J.F. Liebman, L.C. Allen, *J. Am. Chem. Soc.* 92 (1970) 1142.
- [10] B.S. Ault, G.C. Pimentel, *J. Phys. Chem.* 79 (1975) 621.
- [11] W.M. Sun, D. Wu, Y. Li, Z.R. Li, *Chem. Phys. Chem.* 14 (2013) 408.
- [12] Q. Li, R. Li, Z. Liu, W. Li, J. Cheng, *J. Comp. Chem.* 32 (2011) 3296.
- [13] M. Solimannejad, *Chem. Phys. Chem.* 13 (2012) 3158.
- [14] M. Solimannejad, S. Ghafari, M.D. Esrafil, *Chem. Phys. Lett.* 577 (2013) 6.
- [15] M. Solimannejad, Z. Rezaei, M.D. Esrafil, *J. Mol.*

- Mod 19 (2013) 5031.
- [16] M. Solimannejad, Z. Rezaei, M.D. Esrafil, Mol. Phys. DOI: 10.1080/00268976.2013.864426.
- [17] M.D. Esrafil, P. Esmailpour, F. Mohammadian-Sabet, M. Solimannejad, Chem. Phys. Lett. 588 (2013) 47.
- [18] M. D.Esrafil, P. Fatehi, M. Solimannejad, Comput. Theor. Chem. 1022 (2013) 115.
- [19] M.D. Esrafil, P. Juyban, M. Solimannejad, Comput. Theor. Chem. 1027 (2014) 84.
- [20] M.D. Esrafil, P. Esmailpour, F. Mohammadian-Sabet, M. Solimannejad, Int. J. Quantum. Chem. 114 (2014) 295.
- [21] P. Metrangolo, G. Resnati, Science 321 (2008) 918.
- [22] Y. Lu, T. Shi, Y. Wang, H. Yang, X.X. Yan, Luo, H. Jiang, W. Zhu, J. Med. Chem. 52 (2009) 2854.
- [23] R. Cabot, C.A. Hunter, Chem. Commun. 45 (2009) 2005.
- [24] P. Metrangolo, G. Resnati, T. Pilati, S. Biella, Struct. Bond 126 (2008) 105.
- [25] B.K. Saha, A. Nangia, M. Jaskolski, Cryst. Eng. Comm. 7 (2005) 355.
- [26] P. Politzer, J.S. Murray, M.C. Concha, J. Mol. Model 13 (2007) 643.
- [27] P. Auffinger, F.A. Hays, E. Westhof, P.S. Ho, Proc. Natl. Acad. Sci. U.S.A. 101 (2004) 16789.
- [28] A.R. Voth, F.A. Hays, P.S. Ho, Proc. Natl. Acad. Sci. U.S.A. 104 (2007) 6188.
- [29] H. Matter, M. Nazare, S. Gussregen, D.W. Will, H. Schreuder, A. Bauer, M. Urmann, K. Ritter, M. Wagner, V. Wehner, Angew. Chem. Int. Ed. 48 (2009) 2911.
- [30] E. Parisini, P. Metrangolo, T. Pilati, G. Resnati, G. Terraneo, Chem. Soc. Rev. 40 (2011) 2267.
- [31] P. Politzer, P. Lane, M.C. Concha, Y. Ma, J.S. Murray, J. Mol. Model. 13 (2007) 305.
- [32] T. Clark, M. Hennemann, J.S. Murray, P. Politzer, J. Mol. Model 13 (2007) 291.
- [33] P. Politzer, J.S. Murray, T. Clark, Phys. Chem. Chem. Phys. 12 (2010) 7748.
- [34] P. Politzer, J.S. Murray, T. Clark, Phys. Chem. Chem. Phys. 15 (2013) 11178.
- [35] M.D. Esrafil, M. Solimannejad, J. Mol. Model. 19 (2013) 3767.
- [36] J.S. Murray, P. Lane, T. Clark, K.E. Riley, P. Politzer, J. Mol. Model. 18 (2012) 541.
- [37] I. Alkorta, J. Elguero, J.E. Del Bene, J. Phys. Chem. A 117 (2013) 10497.
- [38] J.E. Del Bene, I. Alkorta, J. Elguero, Phys. Chem. A 117 (2013) 6893.
- [39] K.E. Riley, M. Pitonak, J. Cerny, P. Hobza, J. Chem. Theory Comput. 6 (2010) 66.
- [40] S.F. Boys, F. Bernardi, Mol. Phys. 19 (1970) 553.
- [41] P. Su, H. Li, J. Chem. Phys. 131 (2009) 014102.
- [42] E.A.C. Lucken, Nuclear Quadrupole Coupling Constants, Academic Press, London, 1990.
- [43] P. Pyykkö, Mol. Phys. 99 (2001) 1617.
- [44] M.W. Schmidt, K.K. Baldrige, J.A. Boatz, S.T. Elbert, M.S. Gordon, J.H. Jensen, Koseki, S. Matsunaga, K.A. Nguyen, S.J. Su, T.L. Windus, M. Dupuis, J.A. Montgomery, J. Comput. Chem. 14 (1993) 1347.
- [45] A. Bondi, J. Phys. Chem. 68 (1964) 441.
- [46] H. Li, Y. Lu, Y. Liu, X. Zhu, H. Liu, W. Zhu, Phys. Chem. Chem. Phys. 14 (2012) 9948.
- [47] J.C. White, E.R. Davidson, J. Chem. Phys. 93 (1990) 8029.
- [48] P. Valiron, I. Mayer, Chem. Phys. Lett. 275 (1997) 46.
- [49] D. Hankins, J.W. Moskowicz, F.H. Stillinger, J. Chem. Phys. 53 (1970) 4544.
- [50] P. Hobza, R. Zahradnik, K. Muller-Dethlefs, Coll. Czech Chem. Commun. 71 (2006) 443.
- [51] K.E. Riley, J.S. Murray, J. Fanfrlík, J. Řezáč, R.J. Solá, M.C. Concha, F.M. Ramos, P. Politzer, J. Mol. Model. 19 (2013) 4651.
- [52] F.A. Bulat, A. Toro-Labbe, T. Brinck, J.S. Murray, P. Politzer, J. Mol. Model. 16 (2010) 1679.
- [53] P. Politzer, J.S. Murray, M.C. Concha, J. Mol. Model. 14 (2008) 659.